COMPUTATION OF IMPULSE CONDUCTION IN MYELINATED FIBERS; THEORETICAL BASIS OF THE VELOCITY-DIAMETER RELATION

L. GOLDMAN *and* JAMES S. ALBUS

From the Department of Physiology, School of Medicine, University of Maryland, Baltimore, Maryland 21201 and the Video Techniques Section of the Goddard Space Flight Center, Greenbelt, Maryland 20770

ABSTRACT For myelinated fibers, it is experimentally well established that spike conduction velocity is proportional to fiber diameter. However no really satisfactory theoretical treatment has been proposed. To treat this problem a theoretical axon was described consisting of lengths of passive leaky cable (internode) regularly interrupted by short isopotential patches of excitable membrane (node). The nodal membrane was assumed to obey the Frankenhaeuser-Huxley equations. The explicit diameter dependencies of the various parameters were incorporated into the equations. The fiber diameter to axon diameter ratio was taken to be constant, and the internode length was taken to be proportional to the fiber diameter. Both these conditions reflect the situation that exists in real, experimental fibers. Dimensional analysis shows that these anatomical conditions are equivalent to Rushton's (1951) assumption of corresponding states. Hence, conduction velocity will be proportional to fiber diameter, in complete agreement with the experimental findings. Digital computer solutions of these equations were made in order to compute a set of actual velocities. Computations made with constant internode length or constant myelin thickness (i.e., nonconstant fiber diameter to axon diameter ratio) did not show linearity of the velocity-diameter relation.

INTRODUCTION

For the continuous case of the nonmyelinated fiber, the theoretical basis of the conduction-velocity fiber diameter relationship has been well developed (Offner et al., 1940; Rushton, 1951; Hodgkin and Huxley, 1952; Hodgkin, 1954; Pickard, 1966). These treatments all require conduction velocity to be proportional to the square root of axon diameter. Recently, Goldman (1964), from a close examination of cable, spike and dimensional fiber characteristics under stretch, has been able to put the theoretical prediction on a solid experimental footing also.

For myelinated nerve fibers the situation is just reversed. Hence proportionality between spike conduction velocity and fiber diameter has long been experimentally well established (Gasser and Grundfest, 1939; Hursh, 1939; Tasaki et al., 1944;

Berry et al., 1944; see Bullock and Horridge, 1965 for a review), while no really satisfactory theoretical treatment has been proposed. The often cited treatment of Rushton (1951) is strictly limited to fibers in "corresponding states" (scaled proportional to the internode length). This restriction is equivalent to considering only those fibers for which conduction velocity is proportional to internode length. Then, since it is experimentally established that fiber diameter is proportional to internode length, conduction velocity will be proportional to fiber diameter (for this special class of fibers under consideration) (Rushton, p. 108). Huxley and Stampfli (1949) presented a treatment based on a series of extremely simplified models. All of these models neglected both myelin leak (even though it was the very elegant experiments and analyses of these same authors that showed that the myelin leak is substantial) and either nodal resistance and capacitance or myelin capacitance. Offner et al., (1940) also presented a simplified model, but it was equivalent to treating the myelinated fiber as the continuous case.

However, it is possible to treat this problem without any such restricting or oversimplifying assumptions. If a myelinated nerve fiber is regarded as being composed of lengths of passive, leaky cable periodically interrupted by short isopotential patches of excitable membrane, in the manner of FitzHugh (1962), and the appropriate diameter dependencies of the various parameters are incorporated, care being taken to note the empirically correct relationships between internode length and fiber diameter and between the axon diameter to fiber diameter ratio and fiber diameter, then one should have a very accurate representation of a set of myelinated fibers from a single nerve (Huxley and Stampfli, 1949). Note that here specific fiber characteristics are known to be constant with changing diameter. This is in contrast to the usual experimental situation where they are simply assumed to be constant or to vary nonsystematically with diameter.

The system of equations describing such a model system has not been solved analytically (Pickard, 1966) but it may be readily treated using the methods of numerical analysis. Alternatively, a dimensional analysis may be made on this system of equations to see if a suitable change in scaling will produce some simple relationship between velocity and diameter. This article describes the results of just such a dimensional analysis. Digital computer solutions of the equation system were also made in order to obtain a range of computed conduction velocity values. Here use was made of the equations of Frankenhaeuser and Huxley (1964) for reconstruction of the nodal action potential rather than the Hodgkin-Huxley (1952) equations and a scaling factor as done by FitzHugh. Solutions of the Frankenhaeuser and Huxley equations for a propagated action potential have not been previously presented.

THE MODEL SYSTEM

The formal assumptions are similar to those of FitzHugh (1962). The reader is referred to Fig. 1 of FitzHugh for an equivalent circuit representation of a mye-

linated fiber. There is a Ranvier node at the origin ($X = 0$). Other nodes are regularly spaced at an internodal distance which is proportional to the fiber diameter. This is the anatomical relationship found experimentally (Zotterman, 1937; Hursh, 1939; Tasaki et al., 1944; Vizoso and Young, 1948; Thomas and Young, 1949; see also Rushton, 1951). Stimulating current is delivered by an electrode at the zeroth node. The fiber is assumed to extend to plus and minus infinity and to be symmetrical in X around the current passing electrode. The external longitudinal resistance (r_0) was arbitrarily taken to have a very small value compared to any of the internal longitudinal resistances considered. The external current density then should be negligible, shortly after the stimulus has been turned off, and no appreciable error should be introduced by assuming the one dimensional case for cable spread of current through an internode (Clark and Plonsey, 1966).

The internodes are represented by sections of uniform leaky transmission line. Potential distribution in the internode is given by

$$C\partial V/\partial t = \frac{\pi(d/2)^2}{R_i}(\partial^2 V/\partial X^2) - \frac{V}{r} \tag{1}$$

where

$$C = k_1 (\log_e D/d)^{-1} \tag{2}$$

and

$$r = k_2 (\log_e D/d) \tag{3}$$

(the expressions for radial capacitance and leak of a cylinder). Definitions of terms and numerical values of constants used for numerical computation are given in the Appendix.

The time course of potential changes at the isopotential nodes is given by the equations of Frankenhaeuser and Huxley (1964) here reproduced for the readers convenience.

$$\pi dl\, C_m\, dV_j/dt = I_j - \pi dl \left[\bar{P}_{NA}\, hm^2 \frac{EF^2}{RT} \frac{[Na]_0 - [Na]_i\, e^{(EF/RT)}}{1 - e^{(EF/RT)}} + P_K' n^2 \frac{EF^2}{RT} \frac{[K]_0 - [K]_i\, e^{(EF/RT)}}{1 - e^{(EF/RT)}} + \bar{P}_p\, p^2 \frac{EF^2}{RT} \frac{[Na]_0 - [Na]_i\, e^{(EF/RT)}}{1 - e^{(EF/RT)}} + g_L(V - V_L) \right] \tag{4}$$

where

$$dm/dt = \alpha_m (1 - m) - \beta_m m \tag{5}$$

$$dh/dt = \alpha_h (1 - h) - \beta_h h \tag{6}$$

$$dn/dt = \alpha_n (1 - n) - \beta_n n \tag{7}$$

$$dp/dt = \alpha_p (1 - p) - \beta_p p \tag{8}$$

and

$$\alpha_m = 0.36\ (V - 22) \Big/ \left[1 - \exp\left(\frac{22 - V}{3}\right)\right] \tag{9}$$

$$\beta_m = 0.4\ (13 - V) \Big/ \left[1 - \exp\left(\frac{V - 13}{20}\right)\right] \tag{10}$$

$$\alpha_h = 0.1\ (-10 - V) \Big/ \left[1 - \exp\left(\frac{V + 10}{6}\right)\right] \tag{11}$$

$$\beta_h = 4.5 \Big/ \left[1 + \exp\left(\frac{45 - V}{10}\right)\right] \tag{12}$$

$$\alpha_n = 0.02\ (V - 35) \Big/ \left[1 - \exp\left(\frac{35 - V}{10}\right)\right] \tag{13}$$

$$\beta_n = 0.05\ (10 - V) \Big/ \left[1 - \exp\left(\frac{V - 10}{10}\right)\right] \tag{14}$$

$$\alpha_p = 0.006\ (V - 40) \Big/ \left[1 - \exp\left(\frac{40 - V}{10}\right)\right] \tag{15}$$

$$\beta_p = 0.09\ (-25 - V) \Big/ \left[1 - \exp\left(\frac{V + 25}{30}\right)\right]. \tag{16}$$

The boundary and continuity conditions are given by:

$$I_0 = \frac{\pi(d/2)^2}{R_i}\left[r_0 I_e + 2 \lim_{X \to 0} \partial V/\partial X\right] \tag{17}$$

where I_0 (the membrane current at the zeroth node) equals twice the unidirectional internal longitudinal current at $X = 0$, and I_e (the delivered stimulating current) equals twice the total longitudinal current at any X, thus expressing the symmetry condition noted above. Also,

$$\lim_{X \to jL} V(x, t) = V_j(t), \qquad j = 0, 1, 2, 3, \cdots \tag{18}$$

where

$$L = 92D. \tag{19}$$

The proportionality constant of equation 19 was estimated from the data of Dodge and Frankenhaeuser (1959) from *Xenopus* fibers. And,

$$I_j = \frac{\left(\lim_{X \to jL+0} \partial V/\partial X - \lim_{X \to jL+0} \partial V/\partial X\right)\pi(d/2)^2}{R_i}. \tag{20}$$

Initial conditions are listed in the Appendix. Stimulating current $I_e(t)$, was an instantaneously rising current pulse turned on at $t = 0$. For the computer solutions

the duration of the stimulating pulse ranged from 0.02–0.15 msec depending on the fiber diameter.

Note that all constants not defined as functions of D are specific, i.e. diameter independent (see Appendix).

For real, experimental myelinated fibers d/D may be taken as constant over the range of fiber diameters (5–35μ) considered here (Gasser and Grundfest, 1939; Taylor, 1942; Schwarzacher, 1954; Sulzmann, 1959; Dyck and Lofgren, 1966; see also Friede and Samorajski, 1967, for measurements made with the electron microscope). For the toad model fiber treated here (equations 4–16 and 19) 0.7 is probably a good representative value for d/D (Tasaki, 1955; Rushton, 1951). Note that the system should not be very sensitive to small changes in d/D (equations 2, 3). This is the normal case.

An obvious advantage of using a model system is that the contribution of various structural features of myelinated fibers to the velocity-diameter relationship may be readily assessed. Computations were therefore made under the same conditions as above except with L held constant and equal to 2 mm (constant internode length case). This should define the role of the proportionality between L and D found experimentally. Computations were also made with the myelin thickness held constant and equal to 3μ (constant myelin thickness case). L was taken to be equal to $131.4d$. This should assess the significance of the constant d/D found experimentally.

The values of the constants in the Appendix are those for *Xenopus* fibers, the preparation described by the Frankenhaeuser and Huxley equations, whenever the appropriate data was available for them. Some values, mostly pertaining to the internode, were taken from frog fibers. However, the constants for frog axons should not be extremely different from those for toad axons. At any rate the exact values of the constants used should not have any effect on the shape of the velocity-diameter relationship.

DIMENSIONAL ANALYSIS

Since L is proportional to D, θ will be proportional to D if the internode delay time is constant with changing diameter. The following treatment of the problem was proposed to us by R. FitzHugh.

For the normal case the relevant equations are 1, 4, 17, 18, and 20. The others do not depend on fiber geometry. Eliminating I_j between equations 4 and 20, equations 1, 4, 17, and 20 may be written

$$C\partial V/\partial t = KL^2(\partial^2 V/\partial X^2) - V/r \qquad (1')$$

where

$$K = \pi(0.7)^2/4R_i(92)^2$$

$$\pi(0.7)lC_mL/92(dV_j/dt) + \pi(0.7)lLI_r/92$$

$$= KL^2 \left(\lim_{X \to jL+0} \partial V/\partial X - \lim_{X \to jL-0} \partial V/\partial X \right) \qquad (4')$$

where I_r is the nodal membrane current density. And

$$I_0 = KL^2(r_0 I_e + 2 \lim_{X \to 0} \partial V/\partial X). \qquad (17')$$

Now, define the dimensionless variable $\bar{X}$ so that $X = \bar{X}L$. Also, let $I_0 = \bar{I}_0 L$, $I_e = \bar{I}_e/L$, and $r_0 = \overline{r_0}$. Note that for steady propagation, i.e. for times long relative to the duration of the stimulating pulse and for distances electrically far from the origin, the exact form of the transformations on I_0 and I_e will not effect θ. Substitution of the barred terms in equations 1', 4', 17', and 18 eliminates L, and since l is independent of D (Dodge and Frankenhaeuser, 1959), indeed eliminates all geometry-dependent constants from the equation system. The solutions of the equation system, then, for any D will all be of the form

$$V = f(\bar{X}, t). \qquad (21)$$

Since the distance parameter is now scaled relative to L, these solutions may all be made to exactly superimpose for any region of steady propagation. Hence the internode delay time will be constant and θ will be proportional to D. This is in complete agreement with the experimental findings. This result may either be taken as further confirmation of the faithfulness of the model axon or as proof that the experiments did not incorporate some systematic error, depending on one's perspective.

Note that equation 21 taken with the definition of $\bar{X}$, is actually the condition of corresponding states as defined by Rushton. Since this result follows from the most accurate model system of a set of real myelinated fibers that could be constructed, it may be concluded that real fibers are indeed in corresponding states. More specifically, the two empirical morphological relations (L/D and D/d are constants) imply that the fibers are in corresponding states. This provides a physical basis for the purely formal assumption of corresponding states. Since for corresponding states a constant D/d implies a constant L/D (Rushton, equation 5) any two of the three conditions are sufficient to show that θ is proportional to D. Note that it is not necessary to know the specific time or voltage dependencies of the conductance variables for the nodal membrane to obtain this result.

This treatment of course, produces no information as to the exact form of the solution nor can any actual conduction velocity values be obtained. However the model system has been described in sufficient detail to obtain $V(X,t)$ by numerical analysis. The next section describes the results of just such computations.

NUMERICAL COMPUTATIONS

The computing methods were similar to those adopted by FitzHugh. The differential equations were put into a difference form and integrated by a first order Runge-Kutta method. The fiber was sampled at each node and at nine evenly spaced points in between. Δt ranged from 0.05–0.15 $\times$ 10^{-6} sec depending on the value of the cable properties chosen. These time intervals were chosen to insure computational stability. In general as long as $\Delta t \leq 0.3\ (\Delta X^2)\ (r_i + r_0)C$ or in no case was ever greater than 0.15 $\times$ 10^{-6} sec, the cable equation gave a stable solution.

For each diameter fiber, $V(x,t)$ and $V_j(t)$ were computed out to node 20, which was shorted to ground. Conduction velocity was determined graphically for each

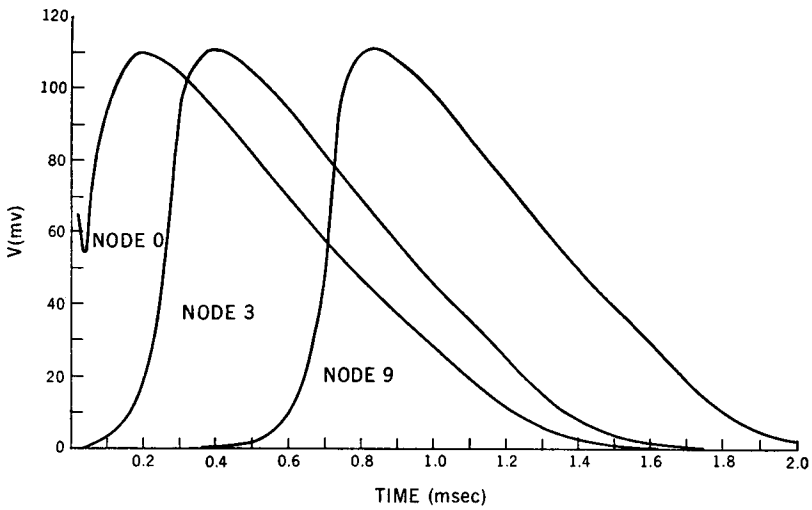

FIGURE 1 Time course of the computed action potentials for a myelinated fiber at nodes 0, 3, and 9. Fiber diameter was taken as 15μ (normal case). Stimulus duration was only 0.01 msec for this computation. Note the changes in the foot of the action potential at node 3 compared to node 0 (see text).

diameter. This conduction distance should satisfy the assumption that the fiber extended to plus and minus infinity.

Computations were made on an IBM 7094 at the Goddard Space Flight Center. A typical running time for a single fiber was 4 min.

Fig. 1 shows the time course of the action potentials computed at nodes 0, 3, and 9 for a fiber with $D = 15\mu$ (normal case). The computed action potential at node 0 may be compared to that shown in Fig. 1 of Frankenhaeuser and Huxley (1964). The slight changes in the foot of the action potential on moving from node 0 to node 3 may be compared to those shown in Fig. 3 of FitzHugh (1962). Note that there is no difference in the form of the action potential at node 3 compared with that at node 9, indicating that at least by the time the action potential has reached node 3, in this case, the time course of the nodal action potential is not affected by the cur-

rent pulse delivered at $X = 0$ or by the second impulse propagating from node 0 to minus infinity. These are the first solutions of the Frankenhaeuser and Huxley equations obtained for a propagated action potential.

Fig. 2 shows the spatial action potentials for a 15μ fiber (normal case) computed at different times after the onset of the simulating current. These curves may be compared with those of Fig. 2 of FitzHugh.

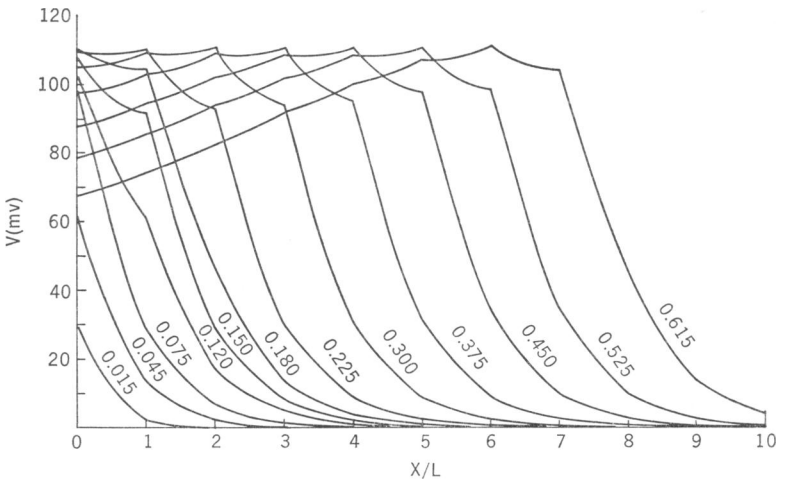

FIGURE 2 Spatial computed action potentials at various times after the onset of the stimulus. Distance from the current-passing electrode is plotted relative to internode length. There is a node therefore at each integer on the X/L axis. $D = 15\mu$ (normal case). The numbers for each curve indicate the time in msec from the onset of the stimulus.

Normal Case

Fig. 3 (solid line) shows the computed conduction velocity as a function of fiber diameter for the normal case. Recall that the normal case should be a faithful representation of a set of myelinated fibers, with constant specific properties, from a single nerve. For the normal case conduction velocity has already been shown to be proportional to fiber diameter, in agreement with the experimental findings. For the normal case, therefore, the entire range of velocities may actually be reconstructed from a single computation. However, θ was in fact computed for several values of D again, of course, showing proportionality between θ and D. It should be emphasized that this computation is logically not an independent treatment from the dimensional analysis and is only presented here for clarity of communication.

Here, and for every diameter fiber considered for each of the three cases, velocity was constant at least by the time the impulse was propagating from node 2 to node 3. All velocities reported as functions of diameter were measured from the time needed for the 50 mv value of the action potential to propagate from node 4 to node 5.

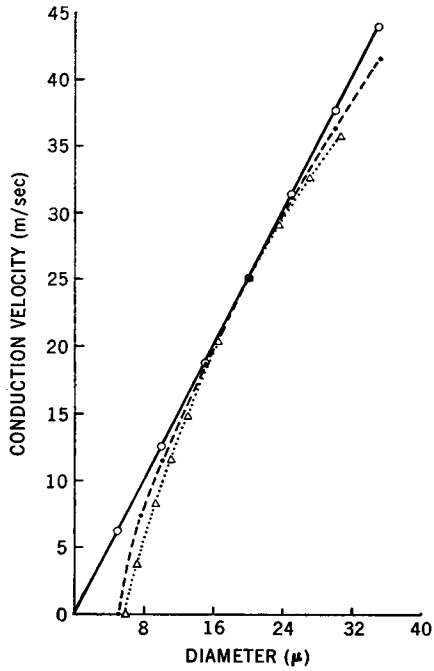

FIGURE 3 Computed conduction velocity as a function of fiber diameter. The solid line and open circles indicate the values for the normal case, the dashed line and filled circles the values for the constant internode length case (L = 2 mm), and the dotted line and triangles those for the constant myelin thickness case ($D - d = 6\mu$).

Values for the constants have been taken from several different types of fibers and r_0 has been arbitrarily set. Hence, the numerical values of θ should not be expected to compare strictly with some particular set of experimental values. However the computed values do agree fairly well with those found experimentally in frog fibers (Bullock and Horridge, 1965).

Constant Internode Length Case

Fig. 3 (dashed curve) shows θ as a function of D for fibers with a constant L (2 mm). Here θ is clearly not proportional to D, again confirming Rushton's insight as to the importance of the proportionality between L and D for the linearity of the $\theta(D)$ relation.

The constant value of L selected means that the $D = 20\mu$ fiber is approximately equivalent to the normal case. For fibers with $D < 20\mu$, θ becomes increasingly less than that for the normal case (even failing to propagate for the 5μ fiber). This is an expected result as the increasing internode length to space constant ratio on decreasing D should eventually reach a point where the maximum amplitude of the signal at any node j will not produce a threshold depolarization at node $j + 1$.

For fibers with $D > 20\mu$, θ becomes less than that for the normal case. This is also an expected result as now there are more (delay producing) nodes per length of fiber as compared to the normal case. As D continues to increase the internode length to space constant ratio will decrease, eventually reaching a point where each node

j is electrically very close to nodes $j + 1$ and $j - 1$. Such fibers in the limit will behave like the continuous case. Hence θ, measured over a distance which is large relative to L, will be proportional to $\sqrt{d}$ (axon diameter) for large D's (see Introduction).

Note that this result (nonlinearity of the $\theta(D)$ relation for constant L) is general. For longer (constant) L's, conduction will fail at a larger D. For smaller L's, the square root relation will be approached at a smaller d.

Constant Myelin Thickness Case

A second structural feature easily examined in the model axon but difficult to manipulate experimentally is d/D. The dotted curve in Fig. 3 shows θ, as a function of D for the condition that d/D varies from 0.368–0.803 (i.e. $D - d$ equals 6μ). As for the constant L case, $\theta(D)$ is not linear.

The $D = 20\mu$ fiber is again equivalent to the normal case. For fibers with $D < 20\mu$, θ is less than that for the normal case. This is true as even though the relatively thicker myelin will reduce both the myelin leak and capacitive current (equations 2, 3), the much shorter internodes for any D (i.e. the same L for a given d as for the normal case) reduce the saltation. In the limit, such fibers will behave much like large D fibers in the constant L case, i.e. adjacent nodes will be electrically (and here also spatially) very close as they will be coupled by very short lengths of virtually non-leaky cable. Very small D fibers then should approach the θ proportional to $\sqrt{d}$ case provided the relative myelin thickness (i.e. D/d) is sufficiently great. This condition was not reached with the myelin thickness selected for the computations shown in Fig. 3 (dotted line).

For $D > 20\mu$, the myelin leak and capacitive currents will become increasingly great, reducing θ as compared to the normal case (Fig. 3). For real fibers the limiting condition of $D/d \rightarrow 1$ means only that the contribution of the myelin to the radial resistance is now negligible compared to that of the membrane itself and the fiber should support action potentials all along the internode and again be in the continuous case. For the modal axon, however, very large D fibers with constant myelin thickness should fail to conduct as the internodes are assumed to be inexcitable (equation 1). The longer internode length at any D compared to the normal case will accelerate the approach to conduction failure. The nonlinearity of the $\theta(D)$ relation for the constant myelin thickness case is, then, also a general result.

SUMMARY

Conduction velocities computed for theoretical myelinated fibers by either dimensional or numerical analysis are proportional to fiber diameter when the model axons are made to resemble real axons as closely as possible. The proportionality between internode length and fiber diameter and the constancy of the axon diameter to fiber diameter ratio found in real fibers are found to be essential to produce

proportionality between fiber diameter and conduction velocity. These structural relations are equivalent to saying that real fibers are in fact in corresponding states as defined by Rushton.

APPENDIX

Variables

t	time
X	distance along axon
jth node	$X = Lj, j = 0, 1, 2, 3 \ldots$
jth internode	$L(j-1) > X > Lj$
L	internode length
$V(X,t)$	potential difference across myelin sheath in internode, inside minus outside
$V_j(t)$	membrane potential difference at jth node
$E_j(t)$	$V_j + E_j$ (0)
$I(X), t)$	outward current density across myelin
$I_j(t)$	outward membrane current at jth node
$I_e(t)$	stimulating current through the electrode at $X = 0$
d	axon diameter (internal myelin diameter)
D	fiber diameter (external myelin diameter)
θ	impulse conduction velocity
C	myelin capacitance per unit length
r	myelin resistance times unit length
r_i	internal longitudinal resistance per unit length

Constants

R_i	axoplasm specific resistance = 110Ω cm (Stampfli, 1952)
k_1	(1.6 $\mu\mu$F/mm) $\log_e$ (1.43) (Tasaki, 1955)
k_2	(290 MΩ mm) $[\log_e (1.43)]^{-1}$ (Tasaki, 1955)
l	nodal gap width = 2.5μ (Dodge and Frankenhaeuser, 1959)
C_m	nodal specific capacitance = 2 μF/cm^2 (Frankenhaeuser and Huxley, 1964)
$\bar{P}_{Na}$	sodium permeability constant = 8×10^{-3} cm/sec (Frankenhaeuser and Huxley, 1964)
P_K'	potassium permeability constant = 1.2×10^{-3} cm/sec (Frankenhaeuser and Huxley, 1964)
P_p	nonspecific permeability constant = 0.54×10^{-3} cm/sec (Frankenhaeuser and Huxley, 1964)
g_L	leak conductance = 30.3 mmho/cm^2 (Frankenhaeuser and Huxley, 1964)
V_L	leak current equilibrium potential = 0.026 mv (Frankenhaeuser and Huxley, 1964)
$[Na]_0$	external sodium concentration = 114.5 mM (Frankenhaeuser and Huxley, 1964)
$[Na]_i$	internal sodium concentration = 13.7 mM (Frankenhaeuser and Huxley, 1964)
$[K]_0$	external potassium concentration = 2.5 mM (Frankenhaeuser and Huxley, 1964)
$[K]_i$	internal potassium concentration = 120 mM (Frankenhaeuser and Huxley, 1964)

F	Faraday's constant
R	gas constant
T	absolute temperature = 293.16°K

Initial Conditions

m_0 = 0.0005
h_0 = 0.8249
n_0 = 0.0268
p_0 = 0.0049
V_j (0) = 0
$V(x, 0)$ = 0, all x
E_j (0) = −70 mv

We thank Dr. R. FitzHugh for many helpful criticisms and Mr. J. A. Muckel for valuable assistance in the running of the computer program. This project was supported in part by PHS Grant NB-06436 from the National Institute of Neurological Diseases and Blindness to L. Goldman. Computer time was furnished by Goddard Space Flight Center.

Received for publication 19 December 1967 and in revised form 8 February 1968.

REFERENCES

BERRY, C. M., H. GRUNDFEST, and J. C. HINSEY. 1944. *J. Neurophysiol.* **7**:103.
BULLOCK, T. H., and G. A. HORRIDGE. 1965. Structure and Function in the Nervous Systems of Invertebrates. W. H. Freeman and Co., San Francisco, Calif. Vol. I.
CLARK, J., and R. PLONSEY. 1966. *Biophys. J.* **6**:95.
DODGE, F. A., and B. FRANKENHAEUSER. 1959. *J. Physiol. (London).* **148**:188.
DYCK, P. J., and E. P. LOFGREN. 1966. *Mayo Clinic Proc.* **41**:778.
FITZHUGH, R. 1962. *Biophys. J.* **2**:11.
FRANKENHAEUSER, B., and A. F. HUXLEY. 1964. *J. Physiol. (London).* **171**:302.
FRIEDE, R. L., and T. SAMORAJSKI. 1967. *J. Comp. Neurol.* **130**:223.
GASSER, H. S., and H. GRUNDFEST. 1939. *Am. J. Physiol.* **127**:393.
GOLDMAN, L. 1964. *J. Physiol. (London).* **175**:425.
HODGKIN, A. L. 1954. *J. Physiol. (London).* **125**:221.
HODGKIN, A. L., and A. F. HUXLEY. 1952. *J. Physiol. (London).* **117**:500.
HURSH, J. B. 1939. *Am. J. Physiol.* **127**:131.
HUXLEY, A. F., and R. STAMPFLI. 1949. *J. Physiol. (London).* **108**:315.
OFFNER, F. A., WEINBERG, and G. YOUNG. 1940. *Bull. Math. Biophys.* **2**:89.
PICKARD, W. F. 1966. *J. Theoret. Biol.* **11**:30.
RUSHTON, W. A. H. 1951. *J. Physiol (London).* **115**:101.
SCHWARZACHER, H. G. 1954. *Acta Anat.* **21**:26.
STAMPFLI,.R 1952. *Ergeb. Physiol.* **47**:70.
SULZMANN, R. 1959. *Jahrb. Morph. Mikr. Anat.* **65**:259.
TASAKI, I. 1955. *Am. J. Physiol.* **181**:639.
TASAKI, I., K. ISHII, and H. ITO. 1944. *Japan. J. Med. Sci. Biophys.* **9**:189.
TAYLOR, G. W. 1942. *J. Cellular Physiol.* **20**:359.
THOMAS, P. K., and J. Z. YOUNG. 1949. *J. Anat. (London).* **83**:336.
VIZOSO, A. D., and J. Z. YOUNG. 1948. *J. Anat. (London).* **82**:110.
ZOTTERMAN, Y. 1937. *Skan. Arch. Physiol.* **77**:123.